Supplemental Material for
"Training Convolutional Networks on Large Weakly Supervised Data"

Armand Joulin* ajoulin@fb.com
Laurens van der Maaten* lvdmaaten@fb.com
Allan Jabri ajabri@fb.com
Nicolas Vasilache ntv@fb.com

Facebook AI Research
770 Broadway, New York NY 10003

1. Introduction

This document contains all supplemental material for the paper "Training Convolutional Networks on Large Weakly Supervised Data". The supplemental material contains six sections: (1) details on the overlap between the CUB200-2011 Birds dataset and the Imagenet ILSVRC2014 dataset; (2) a plot of the word frequency distribution in the Flickr 100M dataset; (3) a section with additional details on the bounds for the approximate multi-class logistic loss of Section 3 in the main paper; (4) additional details on the experimental setup of the transfer learning experiments; (5) additional results of the transfer-learning experiments, comprising all vocabulary sizes; and (6) high-resolution versions of the t-SNE maps presented in the paper.

2. Dataset Overlap

The images in the CUB200-2011 Birds dataset and the Imagenet ILSVRC2014 dataset were partly gathered from the same data sources, such as Wikipedia and Google Image Search. As a result, we expect that there are near duplicates present in these datasets (and possibly also in other datasets that gathered images from these sources). This is problematic, as it means that in transfer learning experiments such as those in [6], some of the images used for testing may in fact also have been used in the training of the feature-production networks—this may lead us to overestimate the performance of such transfer-learning systems.

To investigate the extent of the dataset overlap, we identified near duplicates we use features computed using the quantization procedure from Gong *et al.* [2] and compute an Hamming distance between pairs of images. We then rank these candidate near-duplicate pairs according to this distance. The 8 image pairs with the smallest pairwise distance are shown in Figure 1. We manually inspected the 500 image pairs with the smallest pairwise distance, and counted how many of these image pairs appear to be true duplicates. Using this simple approach, we identified that at least 24 images in the *test set* of CUB200-2011 Birds dataset are also present in the *train set* of Imagenet ILSVRC2014 dataset, i.e. 5% of the images we tested. While our pipeline is imperfect, this number illustrates the danger of evaluating transfer learning across manually annotated datasets gathered from the same source.

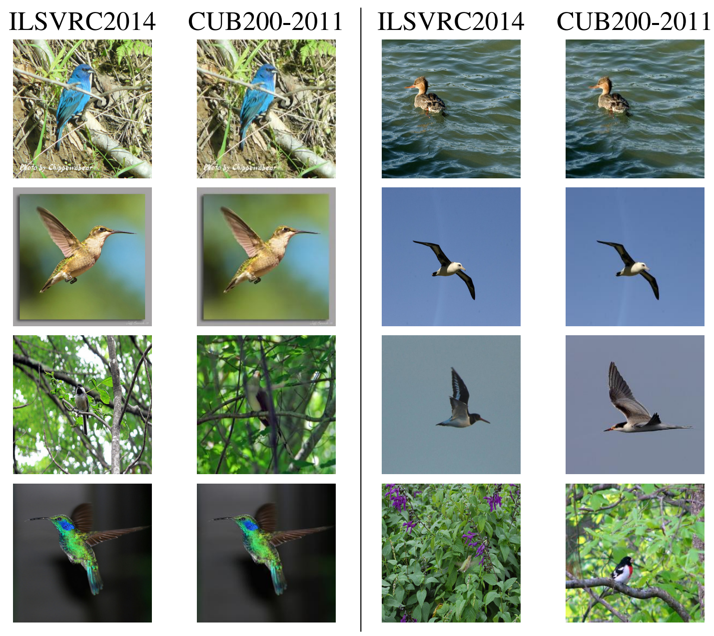

Figure 1. The 8 image pairs with the smallest pairwise distance between the *test set* of CUB200-2011 Birds and *train set* of Imagenet ILSVRC2014. We use the Hamming distance on features computed using the quantization procedure from Gong *et al.* [2]

3. Flickr 100M Word Frequency

Figure 2 shows the word frequency of the 100,000 most common words in the Flickr 100M dataset as a log-log plot: the y-axis shows the log-rank of the words when ranked according to their frequency and the x-axis shows the corre-

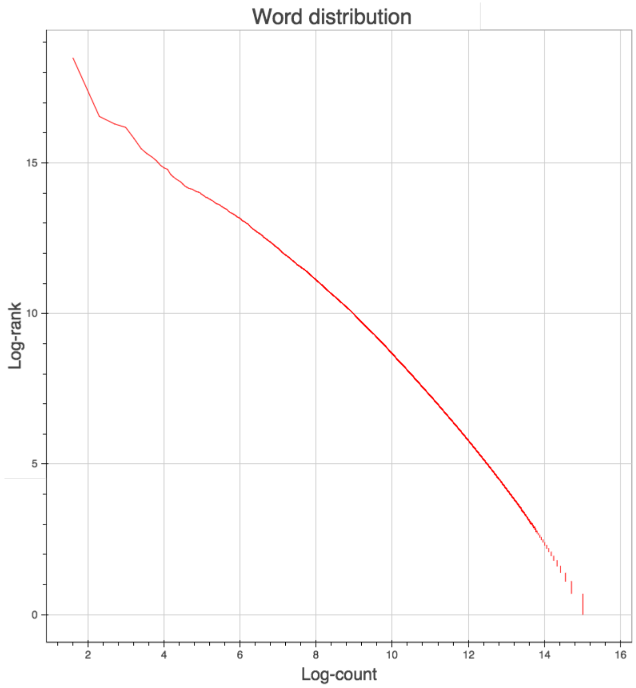

Figure 2. Log-count of words in the Flickr 100M dataset as a function of their log-rank, when words are ranked according to their frequency. The log-log plot is linear, which illustrates that the word frequency distribution is Zipfian.

sponding log-count of the words. The log-log plot is nearly linear, which shows that the word frequencies in the Flickr 100M dataset are, indeed, Zipfian.

4. Bounding the Approximate Multiclass Logistic Loss

This section describes the bounds on the approximate multiclass logistic loss in which the loss is applied only on randomly selected subset of classes in more detail. Our aim is to bound the logistic loss:

$$\ell(\theta, \mathbf{W}; \mathcal{D}) = \frac{-1}{N} \sum_{n=1}^{N} \sum_{k=1}^{K} y_{nk} \log \left[\frac{s_k}{\sum_{k'=1}^{K} s'_k} \right] = \frac{-1}{N} \sum_{n=1}^{N} \sum_{k=1}^{K} y_{nk} \left[\log s_k - \log \sum_{k'=1}^{K} s'_k \right],$$

where we denote $s_k = \exp\left(\mathbf{w}_k^\top f(\mathbf{x}_n; \theta)\right)$. When we randomly sample a subset classes $\mathcal{C}$ (with $|\mathcal{C}| \leq K$) from the set of all K classes, only the partition function $Z = \sum_{k=1}^{K} s_k$ changes. Hence, to bound the multiclass logistic loss, we only need to bound the log-partition function. An upper bound on the log-partition function can trivially be obtained by observing that each element in the sum over K is positive and that $\log(\cdot)$ is a monotonically increasing function:

$$\mathbb{E}\left[\log \sum_{c \in \mathcal{C}} s_c\right] \leq \log\left(\sum_{k=1}^{K} s_k\right) = \log(Z).$$

This bound implies that by randomly subsampling classes, we will never overestimate the loss.

To lower-bound the loss, we first assume that $\forall k : s_k \geq 1$. This assumption can always be satisfied by adding a constant to the term inside the exponential in s_k; this does not change the final loss because the constant is divided out in the loss:

$$\frac{\exp\left(\mathbf{w}_k^\top f(\mathbf{x}_n; \theta) + c\right)}{\sum k' = 1^K \exp\left(\mathbf{w}_{k'}^\top f(\mathbf{x}_n; \theta) + c\right)} = \frac{\exp\left(\mathbf{w}_k^\top f(\mathbf{x}_n; \theta)\right)}{\sum k' = 1^K \exp\left(\mathbf{w}_{k'}^\top f(\mathbf{x}_n; \theta)\right)}.$$

Because we assumed that $\forall k : s_k \geq 1$, we also know that $Z \geq 1$ and thus that $\log(Z) \geq 0$. The positivity of the log-partition function allows us to use Markov's inequality, which states that for any positive random variable x:

$$P(x \geq a) \leq \frac{\mathbb{E}[\phi(x)]}{\phi(a)}.$$

Invoking Markov's inequality on the function $\phi(x) \mapsto \log(x)$ and setting $a = \lambda Z$, we obtain:

$$\mathbb{E}\left[\log \sum_{c \in \mathcal{C}} s_c\right] \geq P\left(\sum_{c \in \mathcal{C}} s_c \geq a\right) \log a = P\left(\sum_{c \in \mathcal{C}} s_c \geq \lambda Z\right) (\log \lambda + \log Z).$$

If we have some knowledge on the distribution of s_k, we can use this to set λ to make the bound as tight as possible. For example, if we assume a uniform distribution over s_k then $\lambda = \frac{C}{K}$ is a good candidate, producing the bound:

$$\mathbb{E}\left[\log \sum_{c \in \mathcal{C}} s_c\right] \geq P\left(\frac{1}{|\mathcal{C}|} \sum_{c \in \mathcal{C}} s_c \geq \frac{1}{K} Z\right) \left(\log\left(\frac{C}{K}\right) + \log Z\right).$$

This bound is particularly interesting because it directly relates the average value of s_c as measured over the set $\mathcal{C}$ to its expected value (indeed, $\mathbb{E}[s_k] = \frac{1}{K} Z$). Also note that the bound becomes exact as $C \to K$.

Using the same setting for λ but assuming that s_k is Gaussian distributed, we obtain:

$$\mathbb{E}\left[\log \sum_{c \in \mathcal{C}} s_c\right] \geq \frac{1}{2} \left(\log\left(\frac{C}{K}\right) + \log Z\right).$$

In this case (and ignoring some constants), the lower bound is at least half of the value of the true loss. Both of these bounds suggest that the approximate loss is, indeed, closely related to the true loss (over all K classes) we wish to optimize. Note that tighter bounds could be obtained by picking λ as a function of Z (since Z is fixed), but, this goes beyond the scope of this paper.

5. Setup of Transfer Learning Experiments

Below, we describe the experimental setup of our transfer-learning experiments for each dataset separately.

MIT Indoor. The MIT Indoor dataset contains $15,620$ images of indoor scenes, comprising a total of 67 categories [5]. The classes are imbalanced, but each class has at least 100 images. The dataset has a fixed subdivision into 80% training images and 20% test images, which we did not use in our experiments. Instead, we performed all experiments via 10-fold cross-validation, using 90% of the images as training and 10% as test data in each run. We measure the accuracy of predicting a class for an image.

MIT SUN. The MIT SUN dataset is a scene dataset; we use the SUN397 release of the dataset, which contains a total of $108,754$ that comprise 397 categories [8]. All our experiments measure classification accuracy, and were performed using 10-fold cross-validation.

Stanford 40 Actions. The Stanford 40 Actions dataset contains images of humans performing 40 different actions [9]. The dataset has a total of $9,532$ images, and there are between 180 and 300 images per action type. Again, we performed experiments using 10-fold cross-validation, measuring classification accuracy.

Oxford Flowers. The Oxford Flowers dataset is a fine-grained classification contains images of 102 different types of flowers [4]. Each dataset contains a total of $8,189$ images, and each class has between 40 and 258 images. Our experiments were performed using 10-fold cross-validation, measuring classification accuracy.

Sports. The Sports dataset contains 300 images of people performing one of 6 different sports actions: "tennis-forehand", "tennis-serve", "volleyball-smash", "cricket-defensive shot", "cricket-bowling", and "croquet-shot" [3]. The classes in this dataset are balanced, and classification accuracies were measured using 10-fold cross-validation.

ImageNet ILSVRC 2014. The ImageNet ILSVRC 2014 dataset contains images of $1,000$ object classes, many of which are fine-grained classes such as dog types and bird types [7]. The data contains a fixed division into a training set of 1281167 images and a validation set of $50,000$ images. The labels of the test are not publicly available, which is why we report validation errors in this paper (we report top-1 classification errors).

Pascal VOC 2007 The Pascal VOC 2007 dataset contains $9,963$ that contain a total of $24,640$ annotated objects [1]. The dataset has a fixed split into 50% training and 50% test data, which we used in all our experiments. As is common in experiments on the Pascal VOC 2007 dataset, we measure the average precision (AP) per class; that is, we rank all images for a particular class and report the area under the precision-recall curve for that class. We also report the mean average precision (mAP), averaged over all classes.

Dictionary size	Model	Indoor	SUN	Action	Flower	Sports	ImNet
1,000	AlexNet	53.19	42.67	51.69	69.72	86.79	35.71
	GoogLeNet	55.56	44.43	52.84	65.80	87.40	37.14
10,000	AlexNet	52.80	40.16	49.51	68.99	88.70	34.28
	GoogLeNet	51.4	40.6	49.52	63.57	86.96	32.02
100,000	AlexNet	53.21	40.21	49.42	70.64	86.96	35.38
	GoogLeNet	–	–	–	–	–	–

Table 1. Classification accuracies on held-out test data of L2-regularized logistic regressors obtained on six datasets (MIT Indoor, MIT SUN, Stanford 40 Actions, Oxford Flowers, Sports, and ImageNet) based on feature representations obtained from convolutional networks trained on the Flickr dataset using $K \in \{1,000; 10,000; 100,000\}$ words and a single crop. Higher values are better.

6. Additional Transfer Learning Results

Table 1 presents the classification accuracies we obtained in the transfer learning experiments with our models for dictionary sizes of $K = 1,000$, $K = 10,000$, and $K = 100,000$. The results show minor differences between convolutional networks trained with different dictionary sizes in the case of Alexnet. For Googlenet, we see a significant change in performance, which may due to the time, it takes to train such a model on larger dictionaries. Table 2 shows the performance of Alexnet on the Pascal VOC 2007 dataset for different dictionary sizes. We observe that the performance becomes slightly worse as the size of the dictionary increase. Table 3 shows the performance of combined GoogLeNet features on the on Pascal VOC 2007 dataset using 10 transformations and a neural network classifier with $4,096$ hidden units.

Finally, Table 4 shows the difference between the one-versus-all logistic loss and the multi-class logistic loss on transfer learning problems. The difference in performance clearly demonstrates the strong performance of the multi-class loss.

7. High-Resolution t-SNE Maps

Figure 3 presents a high-resolution version of the image t-SNE map shown in Figure 4 of the main paper. Figure 3 presents a high-resolution version of the hashtag t-SNE map shown in Figure 6 of the main paper.

Model	Dictionary size																					mAP
AlexNet	1, 000	84.0	72.2	70.2	77.0	29.5	60.8	79.3	69.5	49.2	40.5	54.0	57.1	79.2	64.6	90.2	43.0	47.5	44.1	85.0	50.7	62.4
	10, 000	82.21	69.54	71.50	77.76	31.22	52.75	79.88	60.22	50.04	40.15	51.44	49.48	78.75	68.82	90.44	43.08	50.05	43.12	83.01	50.98	61.22
	100, 000	79.98	67.76	69.80	73.64	24.15	61.55	77.87	57.36	47.52	43.20	51.28	49.32	76.98	66.07	90.36	42.53	51.32	43.21	82.55	48.00	60.22

Table 2. Pascal VOC 2007 dataset: Average precision (AP) per class and mean average precision (mAP) of classifiers trained on features extracted with networks trained on Flickr dataset using $K \in \{1,000; 10,000; 100,000\}$ words. Higher values are better.

Model																					mAP
Combined GoogLeNet	93.07	90.07	91.43	88.78	52.95	85.89	89.58	89.65	60.95	79.66	76.11	89.9	91.34	88.27	89.14	60.42	83.99	68.29	91.83	78.89	82.01

Table 3. Pascal VOC 2007 dataset: Average precision (AP) per class and mean average precision (mAP) for combined GoogLeNet using 10 transformations and a neural network classifier with 4096 hidden units.

Model	Loss	Indoor	SUN	Action	Flower	Sports
AlexNet	Multi-class	53.19	42.67	51.69	69.72	86.79
	One-vs-all	50.70	40.55	48.89	66.96	88.26

Table 4. Comparison between losses on transfer learning problems. Classification accuracies on held-out test data of L2-regularized logistic regressors obtained on six datasets (MIT Indoor, MIT SUN, Stanford 40 Actions, Oxford Flowers and Sports) based on feature representations obtained from convolutional networks trained on the Flickr dataset using $1,000$ words and a single crop. Higher values are better.

References

[1] M. Everingham, S.M.A. Eslami, L. Van Gool, C.K.I. Williams, J. Winn, and A. Zisserman. The pascal visual object classes challenge — a retrospective. *International Journal on Computer Vision*, 111(1):98–136, 2015. 3

[2] Yunchao Gong and Svetlana Lazebnik. Iterative quantization: A procrustean approach to learning binary codes. In *Computer Vision and Pattern Recognition (CVPR)*, pages 817–824. IEEE, 2011. 1

[3] A. Gupta, A. Kembhavi, and L.S. Davis. Observing human-object interactions: Using spatial and functional compatibility for recognition. *IEEE Transactions on Pattern Analysis and Machine Intelligence*, 31(10), 2009. 3

[4] M.-E. Nilsback and A. Zisserman. Automated flower classification over a large number of classes. In *Proceedings of the Indian Conference on Computer Vision, Graphics and Image Processing*, 2008. 3

[5] A. Quattoni and A.Torralba. Recognizing indoor scenes. In *IEEE Conference on Computer Vision and Pattern Recognition*, 2009. 3

[6] A. Razavian, H. Azizpour, J. Sullivan, and S. Carlsson. Cnn features off-the-shelf: an astounding baseline for recognition. In *Computer Vision and Pattern Recognition Workshops (CVPRW)*, pages 512–519. IEEE, 2014. 1

[7] O. Russakovsky, J. Deng, H. Su, J. Krause, S. Satheesh, S. Ma, Z. Huang, A. Karpathy, A. Khosla, M. Bernstein, A.C. Berg, and L. Fei-Fei. Imagenet large scale visual recognition challenge. *International Journal of Computer Vision*, pages 1–42, 2015. 3

[8] J. Xiao, J. Hays, K. Ehinger, A. Oliva, and A. Torralba. Sun database: Large-scale scene recognition from abbey to zoo. In *Proceedings of the IEEE Conference on Computer Vision and Pattern Recognition*, 2010. 3

[9] B. Yao, X. Jiang, A. Khosla, A.L. Lin, L.J. Guibas, and L. Fei-Fei. Human action recognition by learning bases of action attributes and parts. In *International Conference on Computer Vision*, 2011. 3

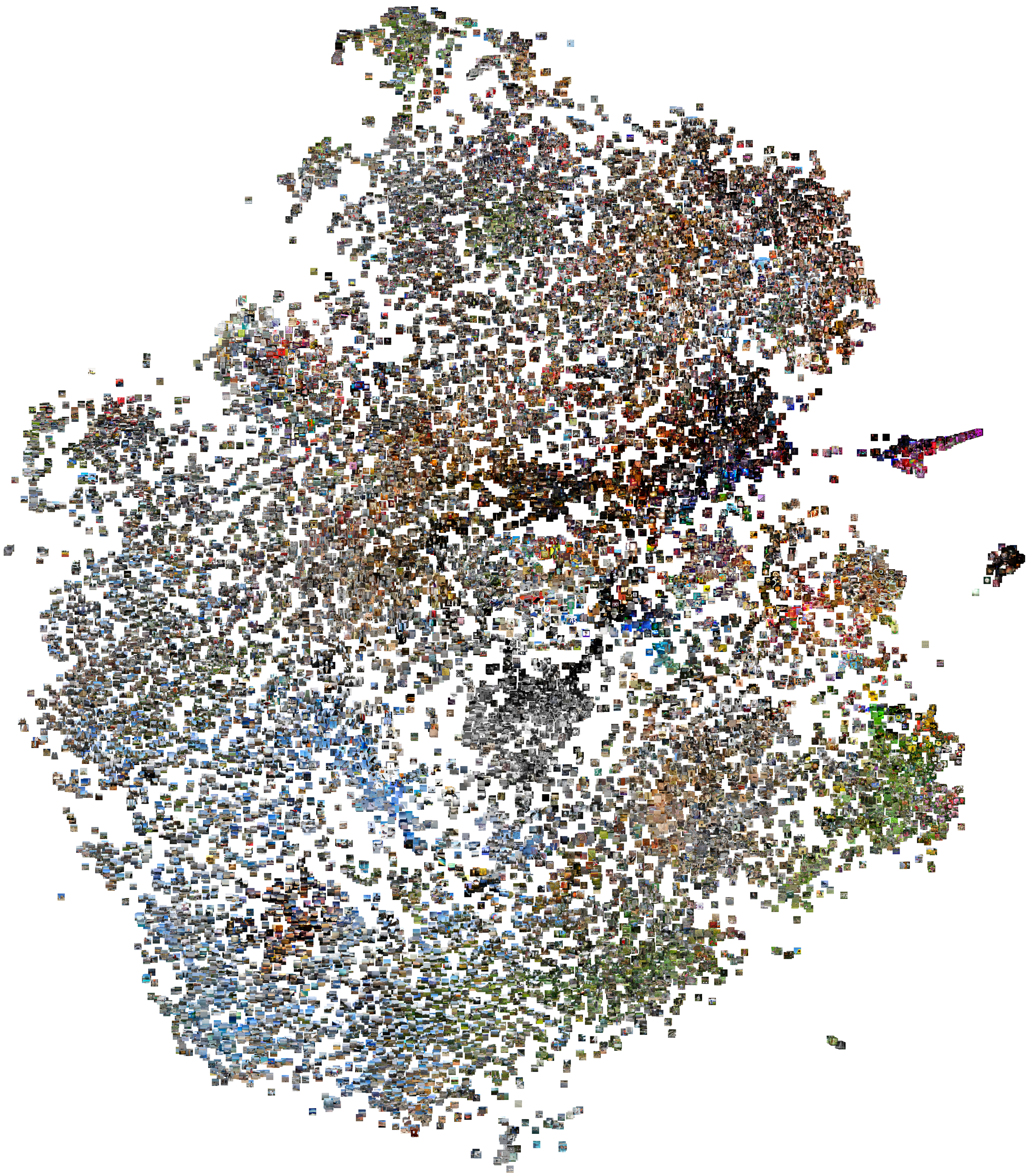

Figure 3. t-SNE map of $20,000$ Flickr test images based on features extracted from the last layer of an AlexNet trained with a dictionary of size $K = 1,000$. Zoom in on the PDF for more detailed views.

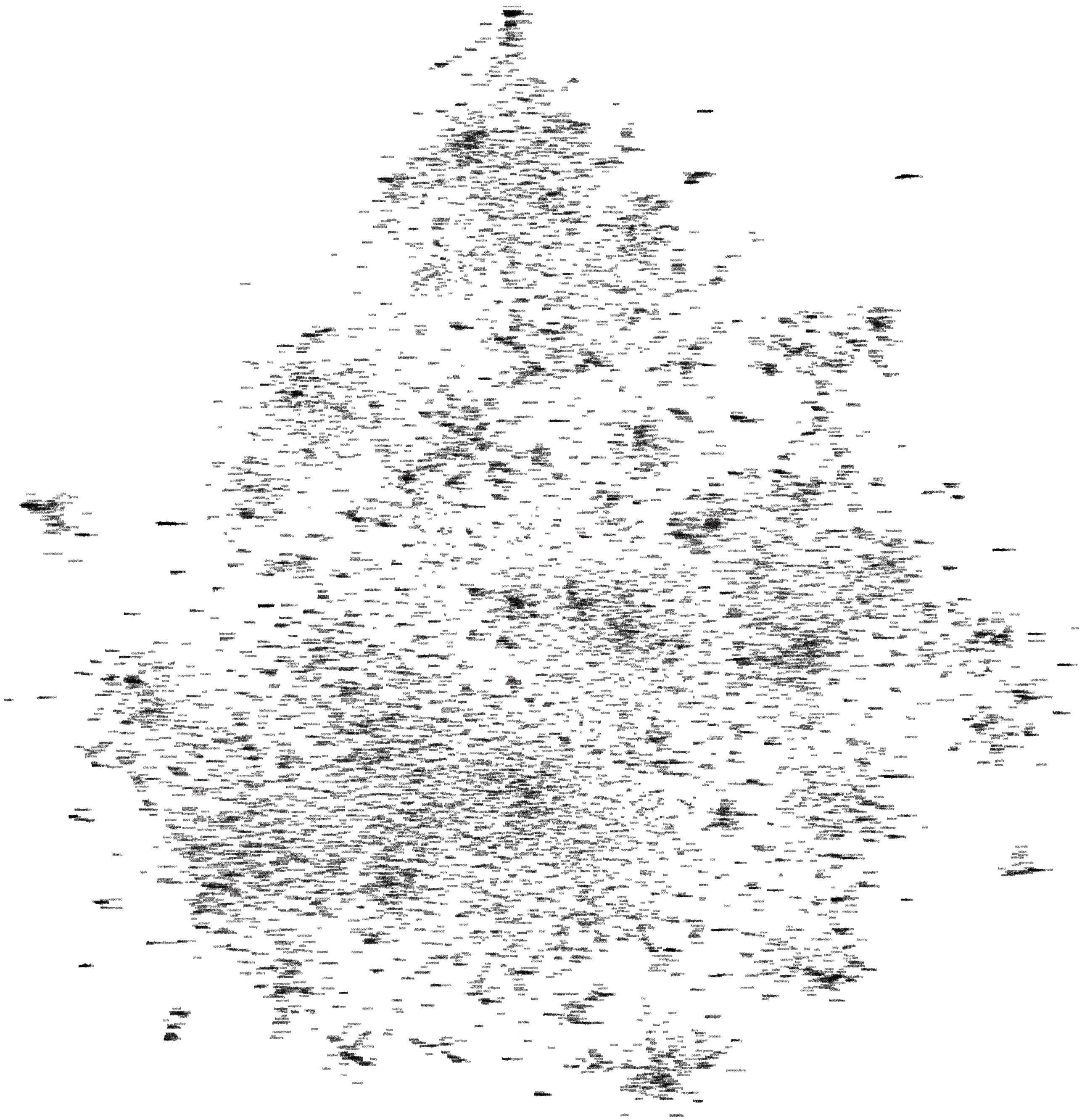

Figure 4. t-SNE map of 10, 000 words based on their embeddings as learned by a weakly supervised convolutional network trained on the Flickr dataset. Zoom in on the PDF for more detailed views.